JOURNAL PRE-PROOF

This is an early version of the article, published prior to copyediting, typesetting, and editorial correction. The manuscript has been accepted for publication and is now available online to ensure early dissemination, author visibility, and citation tracking prior to the formal issue publication.

It has not undergone final language verification, formatting, or technical editing by the journal's editorial team. Content is subject to change in the final Version of Record.

To differentiate this version, it is marked as "PRE-PROOF PUBLICATION" and should be cited with the provided DOI. A visible watermark on each page indicates its preliminary status.

The final version will appear in a regular issue of *Engineering Transactions*, with final metadata, layout, and pagination.

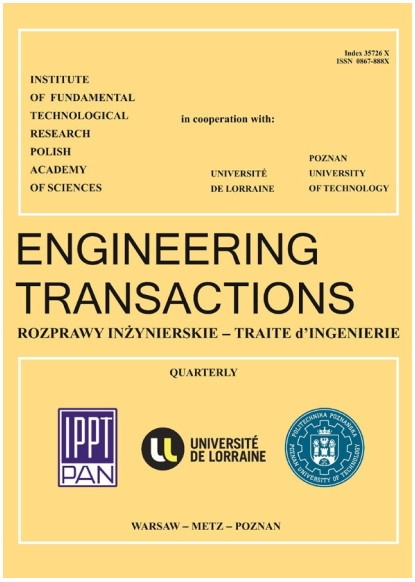

Title: Challenges of Corrosion, Wear, Erosion, and Abrasion in Hydropower Plants: Materials, Modeling, and Mitigation Strategies

Author(s): Harvinder Singh

DOI: https://doi.org/10.24423/engtrans.2026.3574

Journal: *Engineering Transactions*

ISSN: 0867-888X, e-ISSN: 2450-8071

Publication status: In press

Received: 2025-05-16

Revised: 2025-12-31

Accepted: 2026-01-14

Published pre-proof: 2026-01-21

Please cite this article as:

Singh H., Challenges of Corrosion, Wear, Erosion, and Abrasion in Hydropower Plants: Materials, Modeling, and Mitigation Strategies, *Engineering Transactions*, 2026, https://doi.org/10.24423/engtrans.2026.3574

Challenges of Corrosion, Wear, Erosion, and Abrasion in Hydropower Plants: Materials, Modeling, and Mitigation Strategies

Harvinder Singh [1,2]

[1] Department of Mechanical Engineering, Chandigarh Group of Colleges, Landran, Mohali, Punjab, India

[2] Jadara University Research Center, Jadara University, Irbid, Jordan

e-mail: honey.17aug@gmail.com

The chemical, food processing, hydropower, thermal power, and oil industries are among the sectors that frequently face the problems of erosion, abrasion, and corrosion. Pipelines, elbows, reducers, separators, tees, and seals are among the hydraulic devices and pipeline components that are impacted by these difficulties. Silt erosion in turbines and related parts is a major issue in hydropower plants, particularly in Indian hydropower plants where rivers contain hard elements like feldspar, quartz, and other minerals. Remarkably, more than half of the quartz in the silt causes problems in turbines, including sediment erosion, leaks, and secondary flow disturbances. Hydropower plants' total efficiency is ultimately jeopardized by these issues. This paper aims to support scholars and researchers by highlighting the following topics: (i) component failures in impulse and response turbines used in hydropower projects; (ii) different turbine materials and their properties; and (iii) a comparison of several thermal spraying techniques for turbine materials along with numerous numerical models of erosion and abrasion informed by silt characteristics, material properties, and flow phenomena in different hydro-turbines. The study also discusses modeling, pilot plant loops, wear mechanisms, and protective techniques aimed at mitigating wear and safeguarding hydro turbines.

Keywords: thermal spray coatings, erosion, component failure, turbine, hydropower plants.

1. Introduction

Global energy consumption is rising steadily, which is putting tremendous strain on all energy sources. Now, the most widely utilized energy source comes from non-renewable fossil fuels. Fossil fuel supplies could run out by the end of this century, according to estimates [1-3]. Fossil fuel burning also produces toxic byproduct gases that harm the environment. These gases have serious health hazards in addition to their contribution to climate change [4–7]. In response, it is anticipated that soon, renewable energy sources will be essential to supply our expanding energy needs. The basic understanding of using hydropower goes back to the middle of the 1770s, as demonstrated by the work of French engineer Bernard Forest de Bélidor presented the working designs of horizontal and vertical hydraulic machinery [8-10]. However, the first hydropower-driven turbine came into existence in 1878 at Cragside in Northumberland, England, developed by William George Armstrong. Thereafter, the Schoelkopf power station in 1881 and the Edison hydroelectric power plant in 1882 in Appleton, Wisconsin, started to produce electricity from water (http://www.usbr.gov/power/edu/history.html). This was followed by rapid development resulting in around 200 hydropower stations in the U.S. alone by the end of 1889 (http://www1.eere.energy.gov). A remarkable achievement was made in 1928 with the development of Hoover's

Dam, with an initial capacity of 1345 MW. It remained the largest hydropower plant until 1936 when it was surpassed by the 6809 MW Grand Coulee dam in 1942 (www.worldwatch.org). The throttle to produce larger and larger hydropower plants went on and in 1984; a plant having a generation capacity greater than 10 GW came into existence. The Itaipu dam, a joint venture of Brazil and Paraguay with a capacity of 14000 MW, was built. Guri Dam in Venezuela with a capacity of 10200 MW was initiated in 1963, which is presently the third largest dam in the world. Three Gorges Dam in China, currently the largest hydroelectric plant with a capacity of 22500 MW, began working in 2008 (www.hydroworld.com). Today, China is the largest producer of hydroelectricity with 721 terawatt hours generated in 2010. Some countries such as Norway, the Democratic Republic of Congo, Paraguay, and Brazil, are blessed with large water resources with the potential to produce the bulk of their energy requirements from hydropower (www.worldwatch.org). Paraguay generates 100 % of its energy requirements from hydropower. It is also a source of national income for Paraguay, with 90 % of its generation being exported to Brazil and Argentina. Norway also generates 98 % of its energy needs from hydropower. At present, almost 16% of the total generated energy in the entire world is from hydropower. This figure is bound to increase with the initiatives of Asian and African continents, where many of the hydropower resources remain un-harnessed. In 2010, China alone added 16 GW of hydropower generation capacity and plans to add another 140 GW by the year 2015 [8-10].

In the current scenario, India is among the top ten hydroelectric power-generating countries. Out of its total installed capacity of 174 GW in 2011, 21.6 % was contributed by the hydropower mentioned in Fig. 1. By the end of the year 2012, the hydroelectricity generation improved to 39 GW (by ~2GW) (http://powermin.nic.in/). However, the percentage contribution of hydropower appears to have reduced marginally as can be observed in Fig 1, nevertheless, major projects which are under process are surely expected to improve this figure. To mention a few, the hydropower plants at Siang, Upper (11000 MW), and Lower Subansiri (2000 MW) are some of the future projects that could help India gain significant momentum in the field of hydropower generation. In Fig. 2, the trend followed in hydroelectricity generation with the total installed capacity of India since 1947 could be found (http://powermin.nic.in/). It can be observed that hydropower has shown a steady and gradual rise since 1947. Indian rivers have a large potential for hydropower, a significant portion of which remains untapped. Large potential lies in the Brahmaputra, Indus, and Ganga basins, which need to be tapped. In terms of installed generation capacity of hydroelectricity, India stands sixth worldwide (www.worldwatch.org). An idea about the hydropower potential of the country could be obtained from the fact that India has 150000 MW hydropower capacity, which at 60 % load factor amounts to around 84000 MW. Additionally, 15834 MW has been estimated from small hydropower projects. This provides an idea about the growth that could be expected in this sector [5].

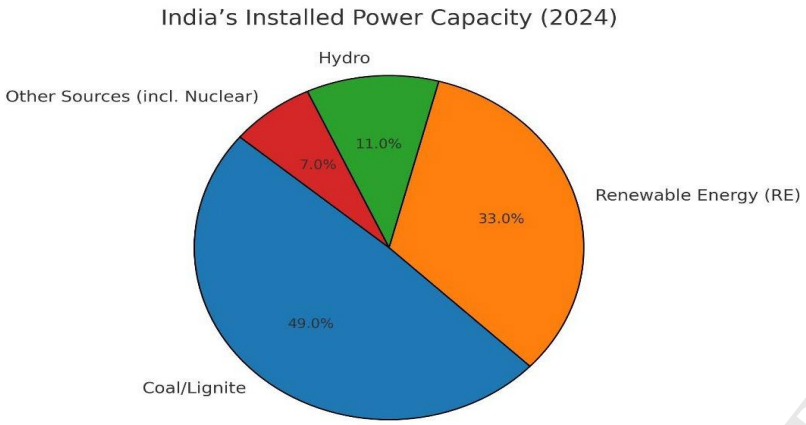

Fig. 1. Distribution of India's power-producing capacity by 2012 makes use of a variety of energy sources, and RES stands for other renewable energy sources.

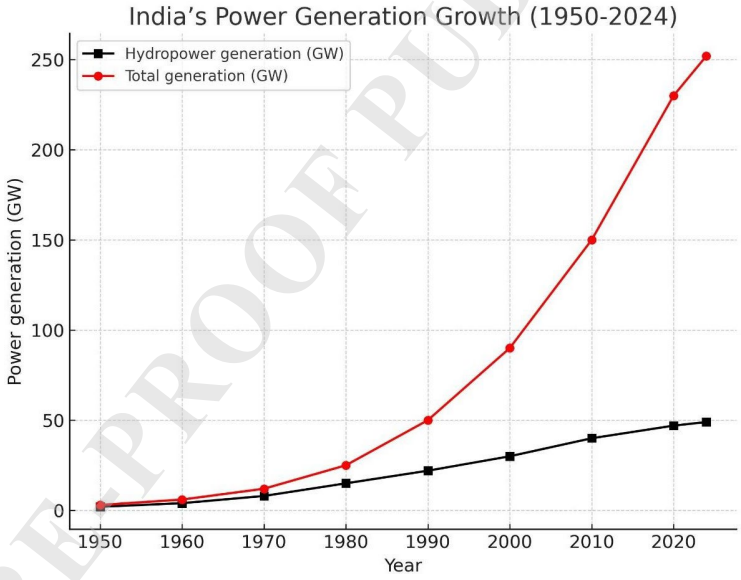

Fig. 2: Variation in hydropower and total generation capacity of India from 1950 to 2024.

2. Problems in hydropower plants

Ideally, a hydropower plant once installed should continue to operate without frequent breakdowns and problems. It is learned that corrosion, a potential hazard for submerged turbines, is not a significant issue anymore for these plants. With the emergence of stainless steel in the early twentieth century, they were readily used in fluid machinery where corrosion was an issue of concern. The addition of chromium (Cr) and nickel (Ni) to iron resulted in steels, which are highly resistant to corrosion. With time, many different stainless steels were developed by varying the proportion of its major constituent elements, viz. Cr and Ni. For hydroturbine applications, steels containing Cr > 12 % are usually recommended [11-12]. Various stainless steels that found their potential use for

hydroturbine applications are listed in Table 1 along with their basic mechanical properties and structure. Among these different steels, 13Cr4Ni, also known by its trade name, CA6NM, is the most employed structural steel for hydroturbine applications. Here the first letter 'C' is a designation, which states that it belongs to the corrosion-resistant family of stainless steels. The letter 'A' gives a rough estimation of the amount of its major constituent elements. Numerals '6' represent 1/100th the percentage of carbon, which is 0.06% in the present case. The last two letters are the representation of the alloying elements, namely, Ni and Mo. The use of highly corrosion-resistant materials such as CA6NM has eliminated the problem of corrosion in hydroturbines. However, wear continues to influence the performance and degradation phenomenon of the turbines [13]. The performance of these hydro turbines is severely impacted by the presence of sand/silt particles in the river waters that flow through the turbines. The loosely held earth particles due to deforestation continue to flow into the rivers with rainwater. Secondly, the young mountains such as the Himalayas do have fragile morphology, because of which the rivers originating from such mountain ranges experience a regular inflow of sand, rock, and debris due to frequent erosion and landslide activities.

Table 1. Properties of different turbine steels [21].

Stainless steel	Tensile strength [MPa]	Yield strength [MPa]	Elongation [%]	Impact strength [J]	Microstructure	Nature
13Cr1Ni	630	470	18	39	Martensite	Hard & brittle
13Cr6Ni	800	550	16	70	Martensite-70 Austenite-30	-
17Cr4Ni	880	650	12	59	Martensite + Ferrite	Hard & ductile
13Cr4Ni	823	686	23	81	Martensite + Austenite	Hard
16Cr5Ni	880	600	21	100	Martensite-65 Austenite-35	Hard & ductile

3. Wear in hydro turbine

Wear is a surface degradation phenomenon resulting from the interaction of solid materials with the surrounding environment. As a result of wear, degradation at the surface of the material occurs either in the form of loss of material or by its relative displacement. Although it is a localized phenomenon at the initial stage, the damage to the surface of the material can exaggerate and coalesce upon continued exposure to degrading environments. This intensifies the damaging process, which further worsens the case and can result in complete stalling of the system [21]. The accumulation of damage and continuous loss of material from the surface can make the exposed component debarred from further service. Wear forms a major portion of the economy of any

country. For example, according to an estimate given in 1965, the loss of 515 million pounds in the United Kingdom alone could have been saved by giving due attention to tribology [22]. In Germany, the total losses due to wear in 1983 were estimated to be around 13 billion pounds. In the United States, the loss due to friction has been estimated to be around $ 100 billion. Depending upon the type of the surrounding environment responsible for the wear of the target surface and the material removal mechanism involved, the process of wear can be categorized into various types as discussed in the next section. Various types of wear mechanisms are described in Fig. 3.

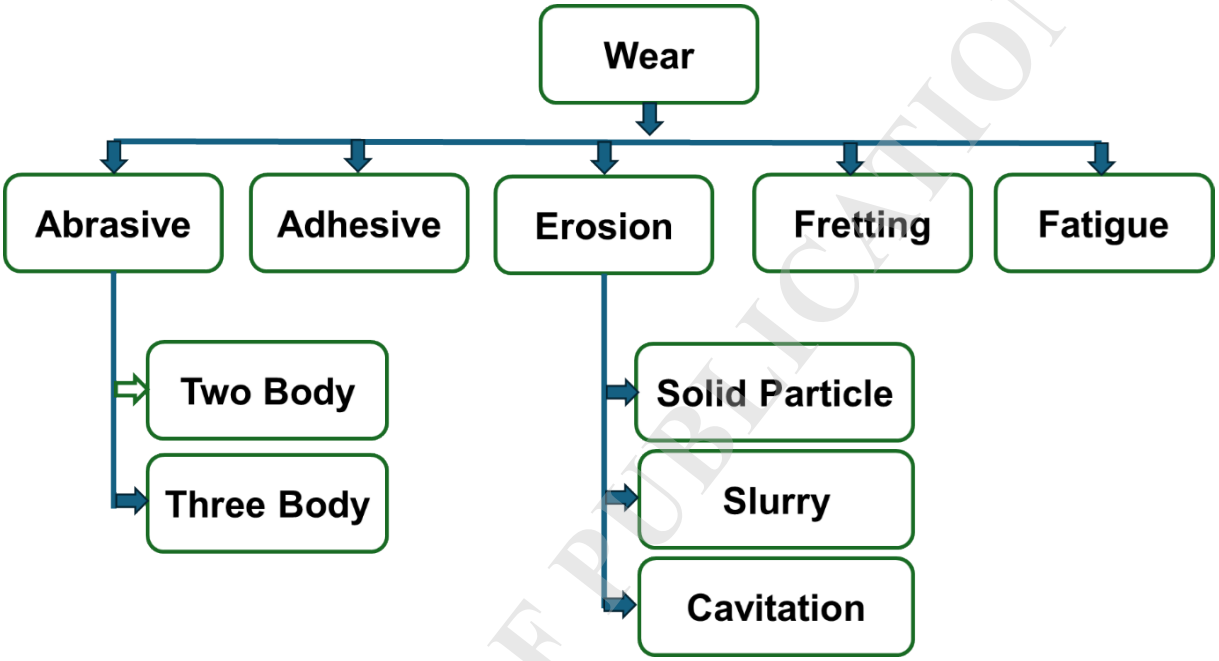

Fig. 3. Describes various types of wear mechanisms.

According to the American Society for Testing and Materials (ASTM) (ASTM-Standard(G40) 2013), erosion is defined as the slow loss of original material from a solid surface that is produced by mechanical contact between the surface and a fluid, a multi-component fluid, or impinging liquid and/or solid particles. As it is clear from the definition itself, due to the impact of the fluid and/or solid, particle and/or both, it results in the mechanical damage of the surface known as erosion. Different forms of erosion shown in Fig. 4 could further help in understanding the different types of erosion. If the erosion is brought on by the impact of solid particles that are entrained in a gaseous medium, this kind of erosion is known as solid particle erosion (SPE). Slurry erosion, on the other hand, is the kind of erosion that occurs when the liquid acts as a carrier fluid rather than gas (SE). Cavitation erosion (CE) and liquid droplet erosion are two other types of erosion that arise from the interaction of the fluid and the solid surface alone (LDE). When CE is present, deterioration occurs because of cavitating circumstances that result from the implosion of cavities or bubbles within liquids that include vapours or mixtures of vapour and gas as shown in Figure 4. It was Rayleigh, who first proposed that the collapse of vapor bubbles resulting in a very high load could initiate the phenomenon of cavitation [23].

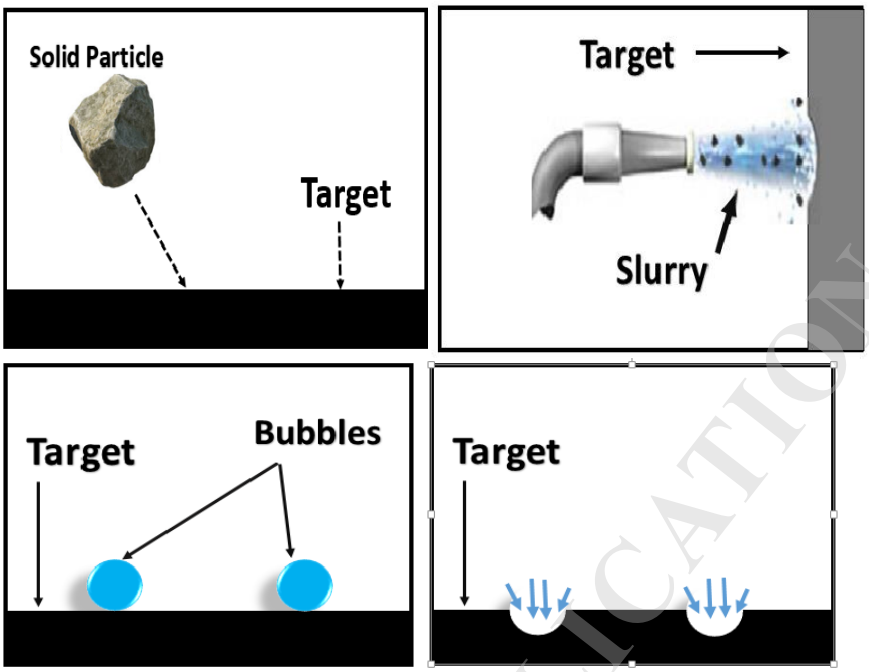

Fig. 4. Schematic describing different types of erosion phenomenon.

4. Impact of erosion on fluid machinery

There are several severely silt-affected hydropower stations in India. The categorization of these plants was made based on the level of impact energy possessed by the silt particles. Plants in which particles having kinetic energy more than 10μJ required repair every second monsoon, whereas repair was required every three to four monsoons wherein particle impact energy was in the range of 5 to 10 μJ. The degraded blade of the 250 MW Francis's turbine at Naptha Jhakri and Baira Siul [24] is shown in Fig. 5. Plants in which the impact energy of the particles was less than 5μJ required repair every seven to eight monsoons. In this categorization, however, no consideration was given to the concentration of the silt particles [24].

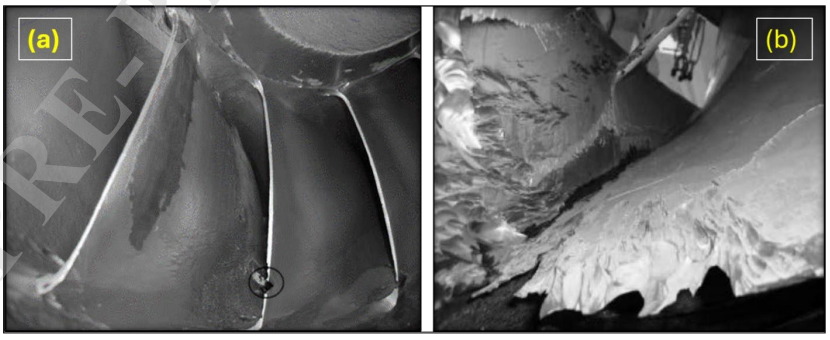

Fig. 5. Degraded turbine blade of 250 MW Francis's turbine at Naptha Jhakri and Baira Siul: (a) degraded turbine blade; and (b) enlarged view of a degraded portion of a turbine blade.

5. Surface modification techniques

For the purpose of altering the surface characteristics of materials, a number of surface modification methods are shown in Fig. 6 [25–26]. There are a few of these processes that pose a threat to the environment [27, 28]. Two of these processes are chemical vapour deposition (CVD) and physical vapor deposition (PVD). Furthermore, using this method makes it challenging to create coatings that are thick. Nevertheless, the heat-affected zone (HAZ) that is generated during processing has an effect on the characteristics of the underlying substrate material in the form of dilution. Other methods, such as laser-assisted surface modification and weld overlay, are very closely related approaches. Thermal spraying is a versatile technique, which can be used to deposit virtually any kind of material to possibly any type of substrate material [29]. It is a versatile technique with the aid of several combinations of materials that could be coated on substrates without altering the properties of the substrate material significantly. Another emerging technique for surface modification is friction stir processing (FSP) [30, 31].

The thermal spraying technique involves spraying molten metal onto a substrate to deposit it. When the coating material is heated to a molten state and sprayed on the substrate at a high velocity with particles as small as a micron, it is first delivered as a powder or wire. Thermal spraying uses combustion or electrical arc discharge for energy. The material is covered by the sprayed particles as they accumulate on the substrate's surface. The porosity, oxide content, macro hardness, surface roughness, and other characteristics of a coating affect its quality. Currently, these coatings are the ones that are most often used. Use of highly erosion resistant materials is restricted by the financial and mechanical strength constraints. The cost of these materials is too high to present a practically viable solution. Secondly, the known erosion resistant materials are typically hard and brittle as a result they would not be able to resist the mechanical stresses induced upon them during working of turbines. Keeping in view of all these facts, the most suitable option, which seems practically viable, is the use of surface modifications. Several surface modifications can be used to alter the surface properties of the existing structural materials to resist the degradation due to erosion, whereas, the underlying structural material can continue to provide required mechanical strength.

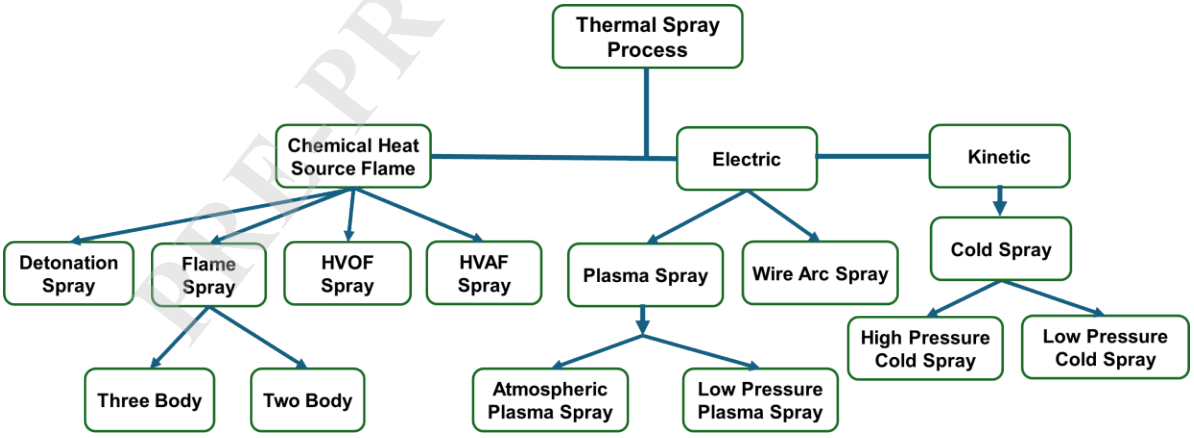

Fig. 6. Classification of thermal spray processes.

5.1 Plasma spraying process

It involves spraying the material on the substrate's surface in the form of a powder or wire while using a plasma torch to heat it to a high temperature. By placing the material in a plasma flame, which melts it, a high temperature is obtained. Then the substrate is approached more quickly by this molten substance. The substance quickly cools when it contacts the substrate, leaving an adhesive coating behind. Plasma gas flows via the anodic nozzle around the cathode, including argon, nitrogen, hydrogen, etc. The plasma starts as a neutral flame, meaning it has no charge. The electric arc descends the nozzle once the plasma is prepared to spray. Because it is electrically non-conducting and increases the plasma arc's velocity. The anode nozzle's cold gas constricts the plasma arc. The powder is heated quickly and propelled toward the substrate as it is fed into the plasma flame, creating an extremely strong and durable coating

5.2 Detonations spraying thermal spray coatings

The Detonation Gun, often known as the D-gun, is the main component of this setup. A long, water-cooled barrel with an open end and a closed end makes up a D-gun. The coating material is delivered into the barrel together with oxygen and fuel gas, and this gas combination is ignited with a spark. The ensuing explosion warms in addition propels powder into the barrel at supersonic speed. After every explosion, the barrel is additionally purged with a pulse of nitrogen. In a second, this procedure is done several times. The heated powder particles move toward the substrate's surface at a very fast speed of roughly 600 m/s. Due to their fast speed, these particles have a high kinetic energy, which when they collide with a substrate, creates an extremely thick and durable coating.

5.3 Wire arc spraying

During this thermal spraying procedure, two metal wires that need to be replaced are fed into the spray cannon one at a time. These wires are charged, and an arc is created between them that burns the incoming wire. The air jet originating from the cannon then carries it away. Wire arc spraying is the procedure by which this molten material is applied to the substrate. This kind of coating is often used for thick coatings [32, 33].

5.4 Flame spraying

As part of this process, the fuel gas is burned in order to melt the spray coating material that is applied to the substrate. This fuel gas is often composed of acetylene or propane that has oxygen added to it. Wire or powder versions of the coating material are often used in the manufacturing process. It is heated before being shot onto the substrate to generate a surface coating.

5.5 HVOF

The decade of the 1980s saw the development of this coating process. During this process, a combustion chamber is filled with a mixture of oxygen and fuel, which may be either gaseous or liquid. The flames of each of them are constantly being kindled and consumed. The heated gas that is produced then travels along a straight segment while being subjected to a pressure of one megapascal (MPa) via a nozzle that converges and diverges. The term "fuel" may refer to either a liquid, such as kerosene, or a gas, such as hydrogen, methane, propane, or acetylene. There is a difference between the speed of sound and the velocity at which the jet leaves the barrel. When injected into a gas stream, a feedstock of powder has the potential to accelerate by up to 800 meters per second. The surface that has to be coated is being approached by a stream of powder and hot gas with rapidly increasing temperatures. As the powder travels through the stream, it partially melts and then settles on the

substrate. This particular coating has a low porosity and a high binding strength in contrast to other kinds of coatings which are available. There is a possibility that HVOF coatings, which are used for ceramic and metal coatings and are often utilized in operations to endure wear and corrosion, may be as thick as 12 millimeters. WC-Co, chromium carbide, alumina, and other powders are often used in the production of these coatings.

5.6 Cold spray (CS)

The cold spray (CS) method uses a de Laval nozzle with a convergent-divergent form to accelerate solid powder particles faster than sound. Speeds between 300 and 1200 m/s are used for ballistic impingement of particles on a suitable substrate. The parameters of the feeding powders, in addition to the form of the nozzle, affect the ultimate temperature and velocity of the particles that are sprayed. These factors are directly connected to the microstructure of the coating as well as its physical and mechanical attributes. It is never the case that the temperature of the gas stream is greater than the point at which the particle material begins to melt. Because it is carried out in the solid state, the coating deposition method has characteristics that are quite different when compared to other standard thermal spray processes. There are now two primary kinds of cold spray systems: high-pressure cold sprays (HPCS), which inject particles from a high-pressure gas source before the spray nozzle throat, and low-pressure cold sprays (LPCS), which inject powder into the diverging region of the spray nozzle. Both of these forms of cold sprays are referred to as cold sprays. The particle speeds that LPCS devices can produce are only 300 to 600 m/s, and they are often portable and much smaller. They are used to apply light materials, and the air or nitrogen that is readily available serves as their normal propellant gas. In systems with high pressure, we use particles with higher density. They typically generate 800 to 1400 m/s particle velocities, are stationary, and employ higher-pressure gases. Lighter gases like nitrogen or helium have been selected as HPCS's propellant gases [34].

6. Protection against erosion

6.1 Use of coatings

The damaging effects of erosion have been discussed in the preceding work. In this part, we would like to elaborate on the various protection schemes used for protection against degradation by erosion. Either by replacing the material with one that has greater erosion-resistant qualities or by simply altering the surface of the components that are already in place, degradation might be decreased. The drawback of the former approach could be the high amount of cost involved in replacing the material with a better one. Furthermore, the requirements for the properties may vary depending on the bulk and the surface. For instance, if the component were to be replaced with a harder material, it would reduce the amount of erosion that occurs. However, the component might lose certain mechanical properties, such as its toughness, ductility, and fracture resistance. With the use of the latter approach, however, we could certainly reduce the cost and retain the desired bulk properties by just modifying the surface properties to our requirements. It has been shown that several of the developing approaches for surface modification, such as cold spray, microwave-aided coatings, and friction stir processing, have demonstrated promising results and have the potential to replace some of the techniques that are now in use.

6.2 Weld overlay technique

It was pointed out by Bonacorso et al. [35] that welding overlays are the most preferred technique for repairing the eroded components of hydroturbines. The presence of complex geometry and unfavorable positions for repairing poses difficulties in the adhesion of the weld to the repaired surface.

Wear studies on 2.5C2.7Cr and 6.7Cr weld overlays produced by MGAW having hardness of 550 and 650 HV were conducted by Dasgupta et al. [36]. It was observed that hard-faced steel performed better in comparison to untreated steel specimens. The direct impact of the variation in the microstructure of the hard-faced overlays and steel on the erosion response and degrading mechanism was observed.

Slurry erosion of metal matrix composite (MMC) coating developed using weld overlays was studied by Flores et al. [37]. Using the plasma transferred arc method, the coating comprised 65 wt. % of WC in Fe-Cr-C matrixes were developed. The effect of addition was clear in the microhardness values showing 1140 HV in comparison to 670 HV of that of the layer formed with any addition. Clearly, the MMC weld overlay showed more than twice the better erosion resistance at 20 C temperature mainly ascribed to the presence of solid parts. Further extending his studies, Flores et al. [38] estimated the enactment of NiCrBSi matrix at high and low levels of alloying elements. Both matrixes were also reinforced with 65 wt. % of WC. NiCrBSi matrix containing higher alloying elements showed somewhat better erosion resistance than its counterpart. The addition of WC helped in improving the erosion performance by 4 to 5 times, however, somewhat better or little better performance was shown among the WC-reinforced matrixes.

Hattori & Mikami [39] evaluated the comparative behavior of cavitation erosion of Stellite 6 and 21 weld overlays with that of SS304 and SS316 on a cavitating jet and ultrasonic rigs. It was observed that Stellite overlays showed 1/7 to 1/13 lower material losses compared to SS304 steel. A direct correlation between erosion with hardness was observed.

Cavitation erosion of NOREM, D-CAV, CaviTec, and Hydroloy 914 advanced weld overlays deposited by GMAW showed erosion in the range of 1 to 2.6 mg/h as compared to that of 3.2 mg/h of SS308 [40]. However, the data presented does not lead to a direct comparison because of the different densities of these materials.

GMAW and SMAW weld overlays of co-alloyed stainless-steel coatings showed a 12 times lower mass loss rate concerning SS316L when tested under cavitating conditions [41]. The mass loss rate was even lower than that of HVOF-coated Stellite 6 steel by a factor of 5. However, no direct correlation with hardness was noticed, showing the dependence on microstructure.

The problem of cavitation-corrosion erosion of Copper-Manganese-Aluminium alloy (CAM) during its service in marine conditions was presented by Li et al. [42]. It was found that the welded zone showed 4 times higher resistance in comparison to the base material. HAZ showed a higher erosion response than that of the weld zone owing to the lack of phase transformation. The benefits of NiTi steel in a cavitating environment have been discussed by Richman et al. [43], however, its high cost and brittle behavior when formed into thick sections limits its practical usage. Two different alloys of NiTi (martensitic and austenitic) were explosively welded onto carbon steel having 0.56 to 0.68 mm thickness. Martensitic NiTi layers performed exceptionally well in comparison to the austenitic counterparts in as-welded conditions. Heat treatment at 500 °C improved the response of austenitic NiTi showing similar mass loss as to that of martensitic. Low-cycle fatigue showed a good correlation with the cavitation erosion behavior of various steels. GTAW TiNi alloy subjected to slurry erosion studies showed a ductile response with maximum mass loss at a 30° impingement angle. AISI 1048 alloy tested under similar conditions showed 50 % more mass loss at the highest level. The better reaction was attributed to this alloy system's excellent work hardening and increased hardness, which came about because

part of the Ti being converted into its oxide during the welding process [44]. Sang & Li [45] studied the response of NiCrBSi based weld overlays produced by flame spray method to their cavitation response. It was found that the presence of uniformly distributed austenitic hard phase led to the highest erosion resistance of Ni60B alloy even higher than that of austenitic stainless steel. CrMnB overlays were tested under cavitation-corrosion conditions owing to their better martensitic transformation capabilities promoting work hardenability [46].

6.3 Thermal spray coatings

According to the literature, surface coatings may help such materials resist slurry erosion. The thermal spraying technologies have garnered a lot of interest lately among the many coating deposition techniques. The behavior of thermal spray coatings' cavitation erosion, however, must be assessed [47–52].

Although WC-based thermal spray coatings may provide substantial slurry erosion resistance [53,54], there is little information on the coatings' cavitation erosion behavior [55] examined the performance of flame-sprayed WC/Co-FeNiCr and Cr2O3 coatings and discovered that microstructural flaws such porosity and partly or completely unmelted particles had an impact on this performance. Although these coatings demonstrated greater confrontation with slurry erosion, they did not function well when exposed to cavitation erosion [56]. Even WC/Co and CrC coatings sprayed with High-Velocity Oxy-Fuel (HVOF) under cavitating erosion conditions sustained substantial damage [56]. The cavitation erosion resistance of the bare steel was not increased by other WC coatings. FeCrSiBMn coatings applied via HVOF were tested, and found that they outperformed ZG06Cr13Ni5Mo martensite stainless steel that had not been coated. The inclusion of complicated carbides and the coatings' increased hardness were credited with improving resistance [57-60].

The study also reveals that Ni-Al2O3-based coatings' slurry/cavitation erosion behavior has not been well studied. Recent research by Hu et al. (2011) examined the effectiveness of cold-sprayed Ni + 40%Al2O3 coatings on Inconel-600 with slurry and cavitation erosion [61]. They demonstrated that, despite the coating's improved slurry erosion performance, its cavitation erosion performance was insufficient. Ni's worse cavitation resistance and lower bonding strength were shown to be the main causes of the coating deterioration. Additionally, the coating's microhardness was only 1.5 to 2.5 times greater than that of the substrate. Ahmed (2002) discovered that contact fatigue loadings are mostly affected by the coating thickness to maximum shear stress depth ratio. According to research, this ratio has to be more than 1.5 for a longer working life [62].

NiTi has been shown to exhibit higher resistance against CE and wear, usually owing to its superelasticity and/or superplasticity properties [63-66]. It was reported that in comparison to solution treatment, NiTi samples aged at 500 °C possessed 8.6 times higher resistance [66]. However, the use of NiTi as a structural material could not be devised as a practical solution owing to its high cost. Moreover, there could be a problem of brittleness in the thick sections. Richman et al. (1995) recommended the coating of NiTi on steel components using an explosive cladding technique to protect them against cavitation erosion [67]. This led to a reduction in the erosion rates of low carbon steel of the order of 30 times in comparison to SS 304 steel. The other conventional coating routes such as fusion welding or thermal spray are not well suited to this composition. During the fusion reaction, brittle phases are introduced and the stoichiometry of NiTi is also affected due to uncontrolled reactions [67]. Thermal spray coatings of NiTi could possess low adherence with steel and lack structural integrity to make them resistible against CE [68, 69]. Although around nine times higher CE resistance of NiTi coatings produced by TiG against that of SS 316 steel has been reported [70], however, this resistance was still significantly lower in comparison to solution heat treated NiTi bulk alloy. This low resistance of NiTi

coating in comparison to bulk NiTi alloy was observed despite the high higher of the former which could be due to the loss of superelasticity during the coating process. Thermal spray coating of NiTi also did not show any further improvement due to the presence of pores as structural defects. The reaction of the powders with the surrounding environment (O2 and N2) results in the formation of brittle phases which eventually lead to the loss of erosion resistance [71]. Furthermore, variation in the erosion rates with Ni percentage in the coating was also reported. Coatings containing Ni higher than the equi- atomic ratio showed higher resistance. After reviewing the relevant literature, it was discovered that there has not been a substantial amount of research conducted to assess the performance of NiTi alloys and coatings with regard to slurry erosion and/or slurry erosion-corrosion [72].

6.4 Ni-alumina-based coatings

Luo Fa (2007) evaluated the toughness and strength of the Ni-Al2O3 composites prepared using Hot Iso-Pressing (HIP) with Ni content varying from 0 to 30 % [73]. When the amount of nickel in the composite grew, it was discovered that the strength of the composite decreased, but the toughness of the composite rose [74]. The maximum hardness reported was 175 HV1.0 for the composite coating having 45 vol. % of hard phase, whereas for the coating with 40 vol. % Al2O3, the maximum hardness was around 650 HK0.1. This variance in hardness was ascribed to the average size of the reinforcing particles (coatings containing much smaller particles, around 1 μm in size), along with the large grain size in the composite of the order of 1mm. Moreover, the microhardness also increased to 524 HV with the rise in alumina content. Similar results have also been reported [75–76]. Szczygieł & Kołodziej (2005) also deposited Ni-6%Al2O3 coating using an electrochemical deposition route and evaluated its corrosion performance [77]. Different coatings were investigated by several researchers [78–86] to determine their microstructure and characteristics. Table 2 provides a review of the various coating materials that may be used to combat erosion.

The coating was found to be successful in enhancing the slurry erosion resistance of Inconel 600. Li et al. (2008) also showed the feasibility of depositing Ni-Al2O3 coatings containing a large volume fraction of hard phased constituents using a cold spray technique [78–79]. The maximum microhardness obtained was only around 173 ± 33 HV0.2, whereas the hardness of the pure Ni coating was found to be around 131 HV0.2. Turunen et al. (2006) deposited nano-crystalline NiAl2O Recently, various researchers [115–119] employed distinct thermal spray coatings to combat corrosion, erosions, and other degradation in different sectors such as thermal power plant, hydroelectric power, gas turbine, aerospace and others. Thus, thermal spray coating has a lot of potential in the coming future [120–125].

Table 2. Summary of past research carried out on different coating materials for combating erosion [87–114].

S. No.	Authors, (Year), and [Ref.]	Coating Materials	Substrate	Process	Coating Thickness (µm)	Avg. Particles Size (µm)	Applications	Remarks/Findings
1	A. Babu et al. (2019) [87]	Ni-SiC	SS316L	Microwave Cladding	500–600	40 ± 5	Hydropower plant	• Without SiC powder Ni cladding shows hardness 360 HV • Achieved the highest cavitation erosion resistance and best combination results with Ni-10 wt% SiC cladding.
2	M. Kazasidis et al. (2019) [88]	Ni and nickel-Inconel 718 powder	Duplex stainless steel	Cold Spray	Up to 3mm	16-45	Hydropower plant	• Achieved 215 HV hardness with Ni-Inconel 718 coatings • Observed an 80 % reduction in overall mass loss and higher cavitation erosion resistance due to the addition of In718.
3	G. Santacruz et al. (2019) [89]	WOKA-3653 (86WC-10Co-4Cr)	AISI 410	HVOF	227	11-45	Hydropower plant	• High slurry erosion resistance. • Tungsten carbide coatings show a 50 % lower erosion rate at an impact angle of 30°
4	A. Bansal et al. (2019) [90]	WC-10Co-4Cr powder	SS 316	HVOF	302	25-40	Hydropower plant	• The modified PTFE shows high hardness varying from 255 to 290 HV • Due to its high hardness, it has a better slurry erosion resistance
5	S. Vignesh et al. (2019) [91]	Iron-based amorphous powder (SHS 574)	AISI 316	HVOF	180–200	15-53	Hydropower plant	• Observed lower erosive wear rate at impact angles 30° and 45° • Observed higher erosive wear rate at 90°
6	V. Sharma et al. (2019) [92]	Ni-40TiO_2 Ni-20TiO_2-20Al_2O_3	13Cr4Ni	HVAF	422 ±10 354 ±10	10-40	Hydropower plant	• Found lower porosity in the range of 0.8 % to 3.6 % for nanostructured composite coatings • Found higher porosity in Ni-20TiO_2-20Al_2O_3 coating than the Ni-40TiO_2 coating

S. No.	Authors, (Year), and [Ref.]	Coating Materials	Substrate	Process	Coating Thickness (µm)	Avg. Particles Size (µm)	Applications	Remarks/Findings
7	G. Nath et al. (2019) [93]	(B4C) (KBF4) (SiC)	13Cr-4Ni	Pack boronizing method	40	-	Hydropower plant	• Found higher erosive wear resistance of 13-4 MSS compared to bare steel due to high hardness (i.e. 2300 VHN) of coating
8	M. Rani et al. (2019) [94]	Ni-Cr-40Al_2O_3	SS316L	HVFS	500-600	50-70 60-90 35-60	Hydropower plant	• The Microhardness of Ni-Cr-40Al2O3 coating was 225 HV but after processing coatings it increased 2 times and increased in fracture toughness
9	Z. Zhang et al. (2019) [95]	Ni60 and WC-17Co	17-4PH stainless steel	APPS HVOF	238-416	140–325 mesh 350–500 mesh	Hydropower plant	• Volume loss is lowered by 50.6 % than the substrate material. WC-17 Co is the best coating material for WDE resistance
10	B. Singh et al. (2019) [96]	Ni+20% Cr7C3	CA6NM	Microwave Cladding	0.92-1.01(mm)	100–150 µm	Hydro power plant	• High erosion resistance It is found that the average weight loss reduced by 45 % of clad samples compared to CA6NM
11	G. Ludwig et al. (2019) [97]	WC10Co4Cr	AISI 410 stainless steel	HVOF	112-155	11–45 µm	Hydro power plant	• Improves the wear properties and high hardness 278 HV with low porosity of 0.3 % to 0.7 % of the deposited coatings

S. No.	Authors, (Year) and [Ref.]	Coating Materials	Substrate	Process	Coating Thickness (µm)	Avg. Particles Size (µm)	Applications	Remarks/Findings
12		Cr3C2–20(80Ni20Cr) WC–Ni	1018 steel	HVOF	221 +16 118 +8	10-45 15-45	Turbine Steel	• Observed 20.5 % improvement in Hardness, i.e., 846 HV to 1020 HV • Observed lowest porosity of about 1 % for Cr_3Cr_2-NiCr cermet coatings
		Cr_3C_2–25NiCr WC-17Co WC-12Co WC-10Co 4Cr Cr_3C_2–40NiCr	1.4571 High-alloyed-steel	HVOF	100-200	20–40		
		Conventional WC–12 Co Nanostructured WC–12 Co CeO2 modified WC–12Co	Stainless steel AISI 304	HVOF	-	15–45 5–45 15–45		
		WC–Co Cr Cr_3C_2–Ni Cr Al_2O_3	S355 steel		163 176 294	15-45 15-45 5-22		
		WC–10 Cr–4 Co	1Cr18Ni9Ti stainless steel	HVOF HVAF	380-420	16-45 5-30		
		Cr_3C_2–Ni Cr Ni–Cr–Fe	1018 steel	APS	200 150	10–90		
13	S. Kaushal et al. (2018) [99]	Cr_3C_2 + 25NiCr	13Cr4Ni	Plasma Spraying	220 + 15	15-45 µm		• Achieved micro hardness up to 1050 VHN of coatings • Decreased cumulative mass loss compared to bare steel
14	V R. Kiragi et al. (2018) [100]	TiAlN coatings	AA1050 AA5083	HVOF	105-150	2-50 µm 2-70 µm	Hydropower plant	• Observed erosion 160 g/min, 195 g/min, and 265 g/min at 75°, 60°, and 30°, respectively

S. No.	Authors, (Year), and [Ref.]	Coating Materials	Substrate	Process	Coating Thickness (µm)	Avg. Particles Size (µm)	Applications	Remarks/Findings
15	D. Kumar et al. (2018) [101]	Al_2O_3-13%TiO_2 and Cr_3C_2–25NiCr	CA6NM	D-gun	-	5 -30 15-45	Hydropower plant	• Found less erosion in Cr_3C_2–25NiCr coating than Al_2O_3-13%TiO_2 • Observed cumulative weight loss 0.1 mg to 1.5 mg in Cr_3C_2–25NiCr coating, and 3.5 mg to 8.5 mg in Al_2O_3-13%TiO_2 coating
16	R.K. Kumar et al. (2017) [102]	WC-CoCr	SS410	HVAF HVOF	380-420	1.2	Hydropower plant	• Found excellent hardness, toughness, and surface residual stress in WC-Co-Cr coating
17	R.K. Kumar et al. (2016) [103]	86WC-10Co4Cr	SS410	HVOF HVAF	410	16-45 20-45	Hydropower plant	• Achieved hardness value up to 1473 HV0.3 with lower porosity 0.3 to 0.9 % • Observed lower weight loss due to cavitation
18	C.A. Widener et al. (2015) [104]	Al 6061 powder	ASTM C633	HPCS	2-8 (mm)	5-68	Al-6061 hydraulic valve actuator	• Found increased in hardness with less porosity varying from 0.93 % to 1.66 %
19	H. Singh et al. (2014) [105]	WC-Co-Cr and Ni-Cr-B-Si	13Cr-4Ni	Plasma Thermal Spray	250-400	5-50	Hydropower plant	• Mass loss increases with an increase in velocity • Found cumulative mass loss 15 mg/cm^2, 12 mg/cm2, 25 mg/cm^2 in WC-Co-Cr, Ni-Cr-B-Si coatings and for bare steel, respectively
20	G. Singh et al. (2013) [106]	Stellite-6 and Cr3C2-25Ni4Cr	13Cr-4Ni	D-gun	100-150	10-53 10-45		• Observed overall specific weight Loss 1897.43 g/m^2 and 345.31 g/m^2 in 13Cr4Ni and Stellite-6 coatings after running 6 h • Observed 5.5 times higher specific weight loss in 13Cr4Ni than in Stellite-6

S. No.	Authors, (Year), and [Ref.]	Coating Materials	Substrate	Process	Coating Thickness (µm)	Avg. Particles Size (µm)	Applications	Remarks/Findings
21	H.S. Grewal et al. (2013) [107]	Ni–Al_2O_3	CA6NM	HVFS	24-684	20-100 20-60	Turbine Steel	• High erosion resistance of coating containing 40wt% of alumina. Uncoated steel shows a 2.2 times lower erosion rate
22	S. Bhandari et al. (2012) [108]	WC-10Co-4Cr	CF8M turbine steel	D-gun	200	15-45	Turbine Steel	• Found reduction in erosion rate of WC-10Co-4Cr coatings • Achieved high hardness of 1120 HV with less porosity of 1 %
23	D. Goyal et al. (2012) [109]	WC–10 Co–4Cr and Al_2O_3+13TiO_2	Turbine steel CF8M	HVOF	1160 830	15-45 10-45	Turbine Steel	• Found high erosion resistance in WC-10Co-4Cr coatings than Al_2O_3+13TiO_2
24	S. Sathik et al. (2012) [110]	Wallex-50 and Tribaloy-700 powders	16Cr-5Ni	Laser surface alloying	600-1000	200	Hydropower plant	• Found excellent ductility and superior toughness even at low temperatures
25	R.C. Shivamurthy et al. (2009) [111]	Cobalt-based Stellite 6 powders and Nickel-based Colmonoy 88	13Cr–4Ni steel	Laser surface alloying (LSA)	300-400	100	Hydropower plant	• Observed 1.25 to 2 times improvement in hardness than substrate material
26	B. S. Mann et al. (2003) [112]	Ti–6Al–4V 17Cr-4Ni PH Steel 12Cr steel	ASTM G73-98	HVOF	250±30	5-50	Steam Turbine blades	• Achieved high hardness and low erosion rate with HVOF coating
27	B. S. Mann et al. (2000) [113]	WC-12Co Cr_3C_2+25NiCr	13Cr–4Ni and T410	D-gun	50-250	5-45	Turbine Components	• It was concluded that the wear rate of hard coatings depends upon the erodent size and amount
28	B. S. Mann et al. (1985) [114]	Composite coating, Ni-Cr-B-Si, WC+Ni-Cr-B-Si	Stainless steel 18-8	Plasma Spraying Process	500 + 25	5-50	Hydropower plant	• Found 1150 HV hardness and 0.73 mg/10h cavitation erosion

7. Conclusions

Hydroelectric power plants in the Himalayan region and other high-sediment mountainous environments face persistent hydro-abrasive erosion, affecting nearly 40 % of installations worldwide. This review synthesizes three decades of multidisciplinary research into a unified framework for understanding and mitigating silt-induced turbine degradation, highlighting that erosion severity is governed by the combined effects of suspended sediment characteristics, hydraulic operating conditions, and turbine material properties. Field observations indicate that unprotected CA6NM components can suffer erosion rates of 0.5 to 3 mm per year, with trailing-edge damage exceeding tip erosion by three to four times. Over time, three complementary mitigation strategies have emerged, including upstream sediment management, advanced protective coatings, and CFD-based turbine design optimization, each offering measurable reductions in erosion and associated maintenance costs. Despite these advances, significant research gaps remain, including large site-to-site variability in erosion calibration despite IEC 62364:2019 standardization, limited understanding of coating durability under transient and seasonal operating conditions, insufficient studies on Kaplan turbine erosion in run-of-river schemes, the early-stage integration of real-time monitoring with machine-learning-based prediction, and the absence of comprehensive life-cycle assessments comparing mitigation pathways. Available evidence shows that integrated approaches combining moderate sediment reduction, design optimization, and selective coating application can reduce material loss by 40 to 60%, lower overall costs by 25 to 35%, and extend maintenance intervals by two to three times. Implementing sediment-aware operational strategies, real-time monitoring, site-specific erosion assessment, cost-optimized coatings, and upstream sediment control can collectively reduce erosion losses by 30 to 50%, extend component life from 3 to 7 years to 12 to 20 years, and significantly enhance the long-term sustainability of hydropower systems worldwide.

7.1 Future research directives

Future research directives derived from this study are as follows:

- Investigate and optimize thermal spraying techniques (air plasma, D-gun, cold spraying, HVOF) to improve the erosion resistance of hydroturbines blade steels.
- Focus on methods to achieve defect-free thermal spray coatings by minimizing porosity, micro-cracks, and through-pores, enhancing coating hardness.
- Focus on methods to achieve defect-free thermal spray coatings by minimizing porosity, micro-cracks, and through-pores, enhancing coating hardness.
- Research rare earth and nanostructured powder materials to optimize coating material combinations for improved performance in hydroturbine applications.
- Study the incorporation of solid lubricants in thermal spray coatings to assess their impact on wear reduction and friction, ensuring cost-effectiveness for specific applications.
- Investigate the effects of additional heat treatment on the microstructure and bonding strength of thermal spray coatings to enhance their corrosion and wear resistance.
- Research techniques to further harden thermal spray coatings and reduce their porosity to increase erosion resistance in practical applications.

The abovementioned research directives highlight key areas for future exploration and development in improving thermal spray coatings for hydropower applications.

Conflict of interest

The author have no financial or proprietary interest in any material discussed in this article.

Funding

This research received no funding.

References

1. Oerlikon. [Internet]. Available from: www.oerlikon.com / metcoinfo.metco@oerlikon.com.
2. Kranzler T. Ensuring product quality through customized materials tests: Classification of materials. Sulz Tech Rev. 2010;25.
3. Sangal S, Singhal MK, Saini RP. Hydro abrasive erosion in hydro turbines: A review. Int J Green Energy. 2018. doi:10.1080/15435075.2018.1431546.
4. Ministry of Power, Government of India. [Internet]. Available from: https://powermin.nic.in.
5. National Hydroelectric Power Corporation (NHPC). [Internet]. Available from: http://www.nhpcindia.com/.
6. Bedi TS, Kumar S, Kumar R. Corrosion performance of hydroxyapatite and hydroxyapatite/titania bond coating for biomedical applications. Mater Res Express. 2019;7:015402. doi:10.1088/2053-1591/ab5cc5.
7. Kumar S, Kumar M, Handa A. Combating hot corrosion of boiler tubes: A study. Eng Fail Anal. 2018;94:379-95. doi:10.1016/j.engfailanal.2018.08.004.
8. Alam T, Islam MA, Farhat ZN. Slurry erosion of pipeline steel: Effect of velocity and microstructure. J Tribol. 2015;138:21604. doi:10.1115/1.4031599.
9. Manisekaran T, Kamaraj M, Shariff SM, Joshi SV. Slurry erosion studies on surface-modified 13Cr-4Ni steels: Effect of angle of impingement and particle size. J Mater Eng Perform. 2007;16:567–72.
10. How Hydropower Plants Work [Internet]. Available from: https://science.howstuffworks.com/environmental/energy/hydropower-plant1.htm.
11. Bitter JGA. A study of erosion phenomena. Wear. 1963;6:169–90. doi:10.1016/0043-1648(63)90073-5.
12. Singh H, Kumar M, Singh R. Development of high-pressure cold spray coatings of tungsten carbide composites. Mater Today Proc. 2023. doi:10.1016/j.matpr.2022.12.210.
13. Singh H, Kumar M, Singh R. Microstructural and mechanical characterization of a cold-sprayed WC-12Co composite coating on stainless steel hydroturbine blades. J Therm Spray Tech. 2022. doi:10.1007/s11666-022-01497-8.
14. Singh H, Kumar M, Singh R. An overview of various applications of cold spray coating process. Mater Today Proc. 2022;56(5):2826-30. doi:10.1016/j.matpr.2021.10.160.
15. Kumar S, Kumar M, Jindal N. Overview of cold spray coatings applications and comparisons: A critical review. World J Eng. 2020;17(1):27-51. doi:10.1108/WJE-01-2019-0021.
16. Franc JP, Michel JM. Fundamentals of cavitation. Dordrecht: Kluwer Academic Publishers; 2004.
17. Santa J, Baena J, Toro A. Slurry erosion of thermal spray coatings and stainless steels for hydraulic machinery. Wear. 2007;263:258–64. doi:10.1016/j.wear.2006.12.061.

18. Chauhan A, Goel D, Prakash S. Erosion behaviour of hydro turbine steels. Bull Mater Sci. 2008;31:115–20. doi:10.1007/s12034-008-0020-6.
19. Amarendra HJ, Chaudhari GP, Nath S. Synergy of cavitation and slurry erosion in the slurry pot tester. Wear. 2012;290–91:25–31. doi:10.1016/j.wear.2012.05.025.
20. Romo SA, Santa JF, Giraldo JE, Toro A. Cavitation and high-velocity slurry erosion resistance of welded Stellite 6 alloy. Tribol Int. 2012;47:16-24.
21. Singh H, Kumar M, Singh R. Combating slurry and cavitation erosion of hydro turbine blades: A study. Int J Adv Sci Technol. 2020;29:5744–55.
22. Singh H, Singh M, Singh R. A comprehensive review of erosion behaviour of hydro turbine blades and their remedies by HVOF process. J Crit Rev. 2020;7(19):ISSN-2394-5125.
23. Singh H, Khosla H, Sidhu TS, Kalsi SBS, Karthikeyan J. Characteristic study of N07718 superalloy surface prepared by cold spray. [Accepted]. 2016.
24. Singh H, Khosla H, Walia GS, Sidhu TS, Kalsi SBS, Karthikeyan J. Characteristic study of cold sprayed N06601 superalloy surface. Surf Eng. 2017. doi:10.1080/02670844.2016.1145600.
25. Pauleau Y. Materials surface processing by directed energy techniques. Elsevier; 2006.
26. Pawlowski L. The science and engineering of thermal spray coatings. 1st ed. 1995.
27. Young MA. Health hazards of electroplating. J Occup Environ Med. 1965;7:348-52.
28. Koropchak JA, Roychowdhury SB. Evidence for aerosol ionic redistribution within aerosols produced by chrome electroplating. Environ Sci Technol. 1990;24:1861-3.
29. Pawlowski L. The science and engineering of thermal spray coatings. 2nd ed. John Wiley & Sons; 2008.
30. Mishra RS, Ma ZY. Friction stir welding and processing. Mater Sci Eng R Rep. 2005;50:1–78.
31. Kumar R, Kumar S. Thermal spray coating process: A study. Int J Eng Sci Res Technol. 2018;7(3):610–7. doi:10.5281/zenodo.1207005.
32. Kumar K, Kumar S, Gill HS. Role of surface modification techniques to prevent failure of components subjected to the fireside of boilers. J Fail Anal Prev. 2022. doi:10.1007/s11668-022-01556-w.
33. Kumar S, Kumar M. Tribological and mechanical performance of coatings on piston to avoid failure: A review. J Fail Anal Prev. 2022;22(4):1346–69. doi:10.1007/s11668-022-01436-3.
34. Bregliozzi G, Di Schino A, Haefke H, Kenny JM. Cavitation erosion resistance of a high nitrogen austenitic stainless steel as a function of its grain size. J Mater Sci Lett. 2003;22(13):981–3. doi:10.1023/A:1024673215823.
35. Bonacorso N, Goncalves Jr A, Dutra J. Automation of the processes of surface measurement and of deposition by welding for the recovery of rotors of large-scale hydraulic turbines. J Mater Process Technol. 2006;179:231–8.
36. Dasgupta R, Prasad BK, Jha AK, Modi OP, Das S, Yegneswaran AH. Slurry erosive wear characteristics of a hard-faced steel: Effect of experimental parameters. Wear. 1997;213:41–6.
37. Flores JF, Neville A, Kapur N, Gnanavelu A. An experimental study of the erosion–corrosion behavior of plasma transferred arc MMCs. Wear. 2009;267:213–22.
38. Flores JF, Neville A, Kapur N, Gnanavelu A. Erosion–corrosion degradation mechanisms of Fe–Cr–C

and WC–Fe–Cr–C PTA overlays in concentrated slurries. Wear. 2009;267:1811–20.

39. Hattori S, Mikami N. Cavitation erosion resistance of stellite alloy weld overlays. Wear. 2009;267:1954–60.
40. Kumar A, Boy J, Zatorski R, Stephenson LD. Thermal spray and weld repair alloys for the repair of cavitation damage in turbines and pumps: A technical note. J Therm Spray Technol. 2005;14:177–82.
41. Boccanera L, Barra SR, Buschinelli AJA, Schwetzke R, Kreye H. Cavitation erosion resistance of Co-alloyed stainless steel weld claddings as compared to thermal sprayed coatings. XXV Encontro Nacional De Tecnologia Da Soldagem, Belo Horizonte; 1999.
42. Li X, Yan Y, Ma L, Xu Z, Li J. Cavitation erosion and corrosion behaviour of copper–manganese–aluminum alloy weldment. Mater Sci Eng A. 2004;382:82–9.
43. Richman RH, Rao AS, Kung D. Cavitation erosion of NiTi explosively welded to steel. Wear. 1995;181–3:80–5.
44. Weng J. Solid/liquid erosion behaviour of gas tungsten arc welded TiNi overlay. Wear. 2003;255:219–24.
45. Singh H. Experimental investigation of WC-12Co cold sprayed: Substrate hardness, bonding mechanism, powder type. Mater Today Proc. 2023. doi:10.1016/j.matpr.2023.01.348.
46. Zheng Y, Luo S, Ke W. Cavitation erosion–corrosion behaviour of CrMnB stainless overlay and 0Cr13Ni5Mo stainless steel in 0.5M NaCl and 0.5M HCL solutions. Tribol Int. 2008;41:1181–9.
47. Cheng FT, Kwok CT, Man HC. Laser surfacing of S31603 stainless steel with engineering ceramics for cavitation erosion resistance. Surf Coat Technol. 2001;139:14–24.
48. Tam KF, Cheng FT, Man HC. Cavitation erosion behavior of laser-clad Ni ± Cr ± Fe ± WC on brass. Mater Res Bull. 2002;37:1341–51.
49. Lo KH, Cheng FT, Kwok CT, Man HC. Improvement of cavitation erosion resistance of AISI 316 stainless steel by laser surface alloying using fine WC powder. Surf Coat Technol. 2003;165:258–67.
50. Duraiselvam M, Galun R, Wesling V, Mordike B, Reiter R, Oligmuller J. Cavitation erosion resistance of AISI 420 martensitic stainless-steel laser-clad with nickel aluminide intermetallic composites and matrix composites with TiC reinforcement. Surf Coat Technol. 2006;201:1289–95.
51. Duraiselvam M, Galun R, Siegmann S, Wesling V, Mordike B. Liquid impact erosion characteristics of martensitic stainless-steel laser clad with Ni-based intermetallic composites and matrix composites. Wear. 2006;261:1140–9.
52. Duraiselvam M, Galun R, Wesling V, Mordike B, Reiter R, Oligmuller J, Buvanashekaran G. Cavitation erosion resistance of Ti6Al4V laser alloyed with TiC-reinforced dual phase intermetallic matrix composites. Mater Sci Eng A. 2007;454–5:63–8.
53. Mann BS, Arya V. An experimental study to correlate water jet impingement erosion resistance and properties of metallic materials and coatings. Wear. 2002;253:650–61.
54. Grewal HS, Bhandari S, Singh H. Parametric study of slurry-erosion of hydroturbine steels with and without detonation gun spray coatings using Taguchi technique. Metall Mater Trans A Phys Metall Mater Sci. 2012;43:3387–401.
55. Singh H, Kumar S, Kumar R, Chauhan JS. Impact of operating parameters on electric discharge machining of cobalt-based alloys. Mater Today Proc. 2023. doi:10.1016/j.matpr.2023.01.234.
56. Santa JF, Espitia LA, Blanco JA, Romo SA, Toro A. Slurry and cavitation erosion resistance of thermal

spray coatings. Wear. 2009;267:160–7.

57. Oka YI, Miyata H. Erosion behaviour of ceramic bulk and coating materials caused by water droplet impingement. Wear. 2009;267:1804–10.
58. Sang K, Li Y. Cavitation erosion of flame spray weld coating of nickel-base alloy powder. Wear. 1995;189:20–4.
59. Kumar S, Handa A, Chawla V, Grover NK, Kumar R. Performance of thermal-sprayed coatings to combat hot corrosion of coal-fired boiler tubes and effects of process parameters and post-coating heat treatment on coating performance: A review. Surf Eng. 2021;37(7):833–60. doi:10.1080/02670844.2021.1924506.
60. Yuping W, Pinghua L, Chenglin C, Zehua W, Ming C, Junhua H. Cavitation erosion characteristics of a Fe–Cr–Si–B–Mn coating fabricated by high velocity oxy-fuel (HVOF) thermal spray. Mater Lett. 2007;61:1867–72.
61. Hu HX, Jiang SL, Tao YS, Xiong TY, Zheng YG. Cavitation erosion and jet impingement erosion mechanism of cold-sprayed Ni–Al2O3 coating. Nucl Eng Des. 2011;241:4929–37.
62. Ahmed R. Contact fatigue failure modes of HVOF coatings. Wear. 2002;253:473–87.
63. Shida Y, Sugimoto Y. Water jet erosion behaviour of Ti-Ni binary alloys. Wear. 1991;146:219–28.
64. Richman RH, Rao AS, Hodgson DE. Cavitation erosion of two NiTi alloys. Wear. 1992;157:401–7.
65. Wu SK, Lin HC, Yeh CH. A comparison of the cavitation erosion resistance of TiNi alloys, SUS304 stainless steel and Ni-based self-fluxing alloy. Wear. 2000;244:85–93.
66. Cheng FT, Shi P, Man HC. Correlation of cavitation erosion resistance with indentation-derived properties for a NiTi alloy. Scr Mater. 2001;45:1083–9.
67. Richman RH, Rao AS, Kung D. Cavitation erosion of NiTi explosively welded to steel. Wear. 1995;181–3:80–5.
68. Jardine AP, Field Y, Herman H, Marantz DR, Kowalsky KA. Processing and properties of arc-sprayed shape memory effect NiTi. Scr Metall Mater. 1990;24:2390–6.
69. Jardine AP, Field Y, Herman H. Shape memory effect in vacuum plasma sprayed NiTi. J Mater Sci Lett. 1991;10:943–5.
70. Cheng FT, Lo KH, Man HC. NiTi cladding on stainless steel by TIG surfacing process Part I. Cavitation erosion behavior. Surf Coat Technol. 2003;172:308–15.
71. Zhou KS, Wang DZ, Liu M. A study of the cavitation erosion behaviour of a Ti-Ni alloy coating. Surf Coat Technol. 1988;34:79–87.
72. Hiraga H, Inoue T, Shimura H, Matsunawa A. Cavitation erosion mechanism of NiTi coatings made by laser plasma hybrid spraying. Wear. 1999;231:272–8.
73. Luo XH, Zhu D, Zhou WC. Mechanical and dielectric properties of Ni/Al2O3 composites. Trans Nonferrous Met Soc China. 2007;17:S1140–3.
74. Levin BF, DuPont JN, Marder AR. The effect of second phase volume fraction on the erosion resistance of metal-matrix composites. Wear. 2000;238:160–7.
75. Tian BR, Cheng YF. Electrolytic deposition of Ni–Co–Al2O3 composite coating on pipe steel for corrosion/erosion resistance in oil sand slurry. Electrochim Acta. 2007;53:511–7.
76. Wu G, Li N, Zhou D, Mitsuo K. Electrodeposited Co–Ni–Al2O3 composite coatings. Surf Coat Technol.

2004;176:157–64.

77. Szczygieł B, Kołodziej M. Composite Ni/Al2O3 coatings and their corrosion resistance. Electrochim Acta. 2005;50:4188–95.
78. Hu HX, Jiang SL, Tao YS, Xiong TY, Zheng YG. Cavitation erosion and jet impingement erosion mechanism of cold sprayed Ni–Al2O3 coating. Nucl Eng Des. 2011;241:4929–37.
79. Li W, Zhang C, Liao H, Li J, Coddet C. Characterizations of cold-sprayed Nickel–Alumina composite coating with relatively large Nickel-coated Alumina powder. Surf Coat Technol. 2008;202:4855–60.
80. Turunen E, Varis T, Gustafsson TE, Keskinen J, Fält T, Hannula SP. Parameter optimization of HVOF sprayed nanostructured alumina and alumina–nickel composite coatings. Surf Coat Technol. 2006;200:4987–94.
81. Hou QY, Huang Z, Wang JT. Influence of nano-Al2O3 particles on the microstructure and wear resistance of the nickel-based alloy coating deposited by plasma transferred arc overlay welding. Surf Coat Technol. 2011;205:2806–12.
82. Guan H, et al. A review of the design, processes, and properties of Mg-based composites. Nanotechnol Rev. 2022;11(1):712–30. doi:10.1515/ntrev-2022-0043.
83. Yang GR, Song WM, Lu JJ, Hao Y, Ma Y. Three-point bending behavior of surface composite Al2O3/Ni on bronze substrate produced by vacuum infiltration casting. J Mater Process Technol. 2008;202(1):195–200. doi:10.1016/j.jmatprotec.2007.08.066.
84. Feng J, Ferreira MGS, Vilar R. Laser cladding of Ni-Cr/Al2O3 composite coatings on AISI 304 stainless steel. Surf Coat Technol. 1997;88:212–8.
85. Feng Q, Li T, Teng H, et al. Investigation on the corrosion and oxidation resistance of Ni–Al2O3 nano-composite coatings prepared by sediment co-deposition. Surf Coat Technol. 2008;202:4137–44.
86. Feng Q, Li T, Zhang Z, et al. Preparation of nanostructured Ni/Al2O3 composite coatings in high magnetic field. Surf Coat Technol. 2007;201:6247–52.
87. Babu A, Arora HS, Singh H, Grewal HS. Microwave synthesized composite claddings with enhanced cavitation erosion resistance. Wear. 2019;422–423:242–51.
88. Kazasidis M, Yin S, Cassidy J, et al. Microstructure and cavitation erosion performance of nickel-Inconel 718 composite coatings produced with cold spray. Surf Coat Technol. 2019;125–195. doi:10.1016/j.surfcoat.2019.
89. Santacruz G, Takimi AS, Camargo FV, Bergmann CP, Fragassa C. Comparative study of jet slurry erosion of martensitic stainless steel with tungsten carbide HVOF coating. Metals. 2019;1–15.
90. Bansal A, Singh J, Singh H. Slurry erosion behavior of HVOF-sprayed WC-10Co-4Cr coated SS 316 steel with and without PTFE modification. J Therm Spray Technol. 2019;1–18.
91. Vignesh S, Balasubramanian V, Sridhar K, Duraisamy DT. Slurry erosion behavior of HVOF-sprayed amorphous coating on stainless steel. Metallogr Microstruct Anal. 2019;8. doi:10.1007/s13632-019-00552-1.
92. Sharma V, Kaur M, Bhandari S. Development and characterization of high-velocity flame sprayed Ni/TiO2/Al2O3 coatings on hydro turbine steel. J Therm Spray Technol. 2019;1–23.
93. Nath G, Kumar S. Slurry erosion behaviour of pack boronized 13-4 martensitic stainless steel for hydro turbine blades. Mater Today Proc. 2018;17380–8.
94. Rani M, Perumal G, Roy M, et al. Post-processing of Ni-Cr-Al2O3 thermal spray coatings through

friction stir processing for enhanced erosion–corrosion performance. J Therm Spray Technol. 2019;1–12.

95. Zhang Z, Zhang D, Xie Y. Experimental study on water droplet erosion resistance of coatings (Ni60 and WC-17Co) sprayed by APS and HVOF. Wear. 2019;432–433:202950.
96. Singh B, Zafar S. Effect of microwave exposure time on microstructure and slurry erosion behavior of Ni + 20% Cr7C3 composite clads. Wear. 2019;426–427:491–500. doi:10.1016/j.wear.2018.12.016.
97. Ludwig GA, Malfatti CF, Schroeder RM, et al. WC-10Co-4Cr coatings deposited by HVOF on martensitic stainless steel for use in hydraulic turbines: Resistance to corrosion and slurry erosion. Surf Coat Technol. 2019;377:124918. doi:10.1016/j.surfcoat.2019.124918.
98. Tiwari A, Seman S, Singh G, Jayaganthan R. Nanocrystalline cermet coatings for erosion–corrosion protection. Coatings. 2019;1–31.
99. Kaushal S, Singh S. Slurry erosion behavior of plasma sprayed coating on turbine steel. Ind Lubr Tribol. 2018. doi:10.1108/ILT-07-2016-0155.
100. Kiragi VR, Patnaik A, Singh T, Fekete G. Parametric optimization of erosive wear response of TiAlN-coated aluminum alloy using Taguchi method. J Mater Eng Perform. 2019;28(2):838–51. doi:10.1007/s11665-018-3816-6.
101. Kumar D. Erosion behaviour of hydroturbine material under air jet erosion tester using D-GUN coating. 6th IEEE International Conference on Smart Energy Grid Engineering; 2018.
102. Kumar RK, Kamaraj M, Seetharamu S, Pramod T, Sampathkumaran P. Effect of spray particle velocity on cavitation erosion resistance characteristics of HVOF and HVAF processed 86WC-10Co4Cr hydro turbine coatings. J Therm Spray Technol. 2016;1–14.
103. Kumar RK, Kamaraj M, Seetharamu S, Kumar S. A pragmatic approach and quantitative assessment of silt erosion characteristics of HVOF and HVAF processed WC-CoCr coatings and 16Cr5Ni steel for hydro turbine applications. Mater Des. 2017;1–51.
104. Singh H, Kumar S, Kumar R, Chohan JS. Impact of operating parameters on electric discharge machining of cobalt-based alloys. Mater Today Proc. 2023.
105. Singh H, Goyal K, Goyal DK. Slurry erosion behaviour of plasma thermal sprayed (50%) WC-Co-Cr and Ni-Cr-B-Si coatings of different thickness on CA6NM turbine steel material. Manuf Sci Technol. 2014;2(4):81–92.
106. Singh G, Bhandari S. Slurry erosion behavior of thermal sprayed Stellite-6 and Cr3C2-25NiCr coatings. Int J Res Mech Eng Technol. 2013;3(2).
107. Grewal HS, Agrawal A, Singh H. Slurry erosion performance of Ni–Al2O3-based composite coatings. Tribol Int. 2013;66:296–306.
108. Bhandari S, Singh H, Kumar H, Rastogi V. Slurry erosion performance study of detonation gun-sprayed WC-10Co-4Cr coatings on CF8M steel under hydro-accelerated conditions. J Therm Spray Technol. 2012;21:1054–1055.
109. Goyal DK, Singh H, Kumar H, Sahni V. Slurry erosion behavior of HVOF sprayed WC–10Co–4Cr and Al2O3+13TiO2 coatings on a turbine steel. Wear. 2012;289:46–57.
110. Sathik S, Periasamy VM, Kamaraj M, Shariff SM. Improvement of slurry erosion wear resistance of 16Cr-5Ni martensite stainless steel by LSA and LTH. J Mater Eng Perform. 2012;22(12):3689–3698.
111. Shivamurthy RC, Kamaraj M, Nagarajan R, Shariff SM, Padmanabham G. Influence of microstructure

on slurry erosive wear characteristics of laser surface alloyed 13Cr–4Ni steel. Wear. 2009;267:204–212.

112. Mann BS, Arya V. HVOF coating and surface treatment for enhancing droplet erosion resistance of steam turbine blades. Wear. 2003;254:652–667.

113. Mann BS. High-energy particle impact wear resistance of hard coatings and their application in hydroturbines. Wear. 2000;237:140–146.

114. Mann BS, Krishnamoorthy PR. Cavitation erosion characteristics of nickel-based alloy-composite coatings obtained by plasma spraying. Wear. 1985;103:43–55.